Simulation of the ASDEX Divertor Performance after Hardening

W. Schneider, K. Lackner,
J. Neuhauser, R. Wunderlich

IPP 5/5 May 1985

MAX-PLANCK-INSTITUT FÜR PLASMAPHYSIK

8046 GARCHING BEI MÜNCHEN

MAX-PLANCK-INSTITUT FÜR PLASMAPHYSIK

GARCHING BEI MÜNCHEN

Simulation of the ASDEX Divertor Performance after Hardening

W. Schneider, K. Lackner,
J. Neuhauser, R. Wunderlich

IPP 5/5 May 1985

Die nachstehende Arbeit wurde im Rahmen des Vertrages zwischen dem Max-Planck-Institut für Plasmaphysik und der Europäischen Atomgemeinschaft über die Zusammenarbeit auf dem Gebiete der Plasmaphysik durchgeführt.

IPP 5/5

W.Schneider
K.Lackner
J.Neuhauser
R.Wunderlich

Simulation of the ASDEX-Divertor Performance after Hardening

Abstract

Two combined computer models - a fluid description of the plasma scrape-off layer (SOLID) and a Monte-Carlo code for the neutral gas dynamics (DEGAS) - are used to assess changes in the divertor performance expected from the modifications in geometry needed for hardening the ASDEX divertor chamber for long-pulse, high-power heating. Stand-alone DEGAS calculations with assumed fixed scrape-off plasma parameters predict a doubling of the neutral escape probability, which, however, still remains so low, that achievement of the high divertor recycling regime can be expected over roughly the same operational regime as before modifications. This conclusion is also supported by fully self-consistent calculations with the combined model. Due to the reduced divertor volume, a significant reduction is predicted in the divertor time constant, which is expected to affect transient phenomena.

1. Introduction

The axially symmetric divertor tokamak ASDEX, operated at IPP Garching, has successfully demonstrated the efficiency of the poloidal divertor for density and impurity control over a wide range of plasma parameters (see /1/). The high recycling divertor regime was obtained in Ohmic discharges /2/ as well as with additional heating in the MW range for a heating pulse duration of a few hundred milliseconds /3/. The additional heating will be extended in the near future to about 6 MW for 2 to 6 seconds (depending on the cooling scenario). Since the deposited energy will be increased by more than an order of magnitude, a "hardening" of the divertor chamber is mandatory, in order to avoid severe damage of the target plates and adjacent chamber walls /4/. Figure 1 shows the new divertor inserts designed for high power and energy load (Fig. 1b) in comparison to the present geometry (Fig. 1a). Concerning divertor physics the most obvious change occurs with respect to the active divertor chamber volume, which is no longer represented by the whole upper (and lower) dome of the vacuum vessel as in the original design. Massive walls, which can be actively cooled, are introduced quite close to the divertor plasma fan (heavy lines in Fig. 1b) with only a small toroidal gap at the top and quite narrow poloidal slits in the walls. In this way, the main recycling volume is reduced to the immediate vicinity of the plasma fan. As a consequence, the neutral particle orbits, the number of wall reflections before re-ionization or escape into the pumped dome or the main chamber etc., are strongly changed. On the other hand, the poloidal magnetic field topology is essentially unchanged, which means that there is still an appreciable compression of flux surfaces at the divertor entrance and a rather narrow slit geometry can be retained. (This is one essential difference with respect to the forthcoming ASDEX Upgrade /5/ which has an "open" divertor geometry similar to that envisaged for INTOR or a reactor.)

In this paper we present a numerical study of the divertor recycling for various geometries and plasma regimes representing typical

(a)

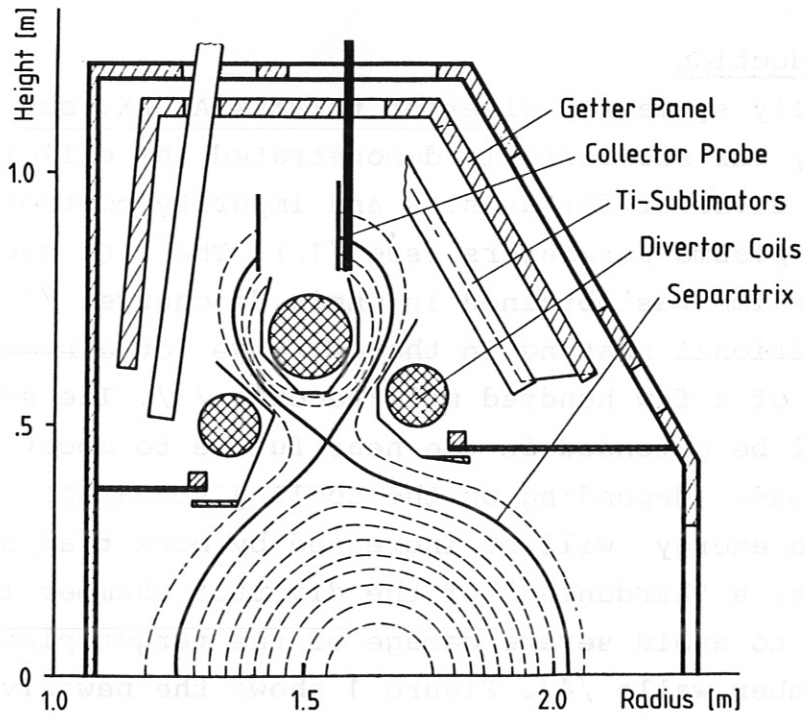

(b)

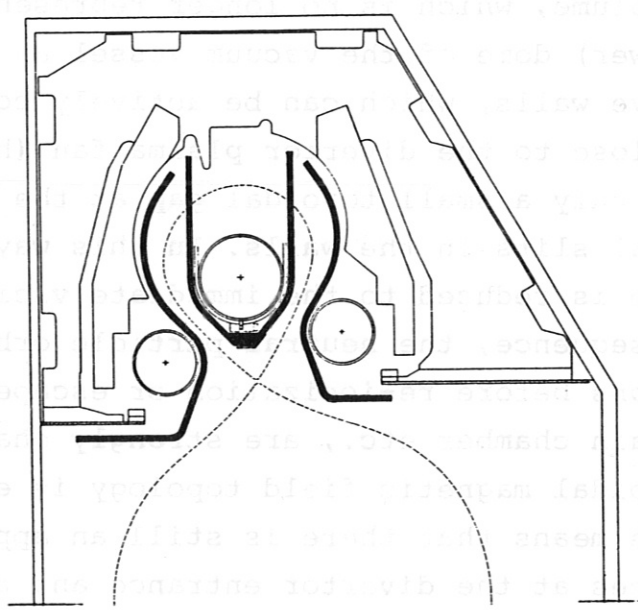

Fig. 1: ASDEX divertor geometry
a) before, and
b) after hardening

ASDEX situations before and after hardening. Two intermediate fictitious cases are included in order to separate effects of different physical origin.

The 1D hydrodynamic code SOLID /6/ coupled with the 2D Monte Carlo neutral gas code DEGAS /7/ is used. We emphasize that it is not the intention of this report to reproduce specific experimental discharges in detail. This has been done elsewhere /6,12/, and is being continued. Here, our main interest is devoted to changes of the divertor recycling pattern if the geometry is altered, keeping the plasma parameters unchanged as far as possible. Typical quantities to be checked are the resulting atom and molecule densities in the divertor, the hydrogen flux pumped or escaping through the entrance slits, the associated time constants, the particle flux amplification and so on. A crucial question is whether a high recycling divertor action can still be obtained with the modified divertor for all bulk plasma parameters of interest at ASDEX.

2. Model

The plasma dynamics in the scrape-off layer, the neutral particle behaviour in the divertor chamber, and, the interaction of the plasma with the neutral gas are described by the combination of two codes: SOLID /6/ calculates the plasma, mass- and energy transport along the field lines from midplane onto the target plates, using a two-temperature fluid model. The neutral gas distribution in the divertor chamber is calculated by the Monte-Carlo code DEGAS /7/, modelling realistic wall and plasma geometries in the poloidal plane. Perfect rotational symmetry with respect to the major torus axis is assumed; i.e. plasma and neutral gas distribution are 2D axisymmetric, but, nevertheless, individual neutral particle orbits must be followed in 3D by DEGAS.

Since SOLID solves a 1D model along the field lines only, we have to prescribe the density and temperature profiles across the field lines in order to define a 2D plasma distribution as input for DEGAS. We assume an exponential decay of the plasma parameters per-

pendicular to the field lines, using typical experimental decay lengths of 2 cm for the electron density and 1.5 cm for the temperatures at the midplane.

Away from the midplane the perpendicular scale lengths are varied according to the local poloidal flux compression. Based on these plasma profiles DEGAS calculates distributions of atomic and molecular neutral densities and temperatures; furthermore the ionization rate, the power losses from the electrons (ionization, radiation, dissociation) and ions (cx-terms) are calculated. These 2D quantities are integrated across the field lines and - after some smoothing along the field lines - are taken over by the 1D SOLID as particle sources and energy sink terms.

This procedure (an improved version of that described in ref. /6/) is iterated. In order to get a stationary solution, the total particle flux ϕ_3 onto the target plates is kept fixed. This means that the net charged particle flux ϕ_1 from the bulk plasma into the scrape-off layer (and finally into the divertor) is adjusted so as to replace exactly the divertor losses caused by gettering at the walls (ϕ_{gett}) and by particles escaping into the main chamber through the divertor slits (ϕ_{exit}). The ionization or recycling flux ϕ_2 in the divertor clearly is not a net particle loss. In the high recycling regime the relative magnitude of these fluxes is $\phi_3 \gtrsim \phi_2 \gg \phi_{gett} \sim \phi_{exit} \sim \phi_1$, and for a stationary state $\phi_3 - \phi_2 = \phi_1 = \phi_{gett} + \phi_{exit}$ holds.

Prescribing the target flux ϕ_3 and in addition the total power input ϕ_E into the scrape-off layer means that the plasma temperature near the target plates is also nearly fixed, since it is roughly proportional to ϕ_E/ϕ_3 /8/. For a constant ratio ϕ_E/ϕ_3, the divertor density increases with increasing ϕ_3 (and ϕ_E). Hence the two input parameters ϕ_E and ϕ_3 determine the divertor plasma within narrow limits, while the other fluxes can adjust themselves freely according to the divertor geometry, gettering efficiency etc.

This iteration procedure is quite adequate for our present purpose, where we try to compare the neutral gas divertor geometries, keeping at the same time the divertor plasma parameters fixed as far as possible. In fact, for the first DEGAS iteration identical plasma profiles can be provided as input by SOLID for all cases so that direct comparison of various neutral gas quantities is possible after this step. Of course, this is not yet a selfconsistent solution, but the final state after several iterations is not much different as long as the geometry and plasma data allow for a high recycling situation. (Much stronger changes in the divertor plasma during the iterations occur, if we fix ϕ_1 instead of ϕ_3, since variations in the small fluxes ϕ_{gett} and ϕ_{exit} cause large variation in ϕ_3 and hence in the divertor plasma parameters.)

Experimentally one cannot directly control the target flux ϕ_3. Usually the heating power is given (related to ϕ_E) and the average bulk plasma density $\bar{n}$ is feedback controlled. However, these two parameters do not yet fix the scrape-off layer characteristics. These depend also on the geometry ("open" or "closed" divertor) and on particle sources and sinks (gettering or gas puffing in the main chamber or in the divertor) /19/. But once a quasi-stationary state is obtained in experiment or simulation, the question how this state has been reached is clearly irrelevant, except if it can be shown that the simulated equilibrium is not accessible from reasonable starting conditions. An interesting problem would arrise in case of bifurcation of equilibria and their stability, where the particular branch realized would probable depend in fact on the parameters kept fixed. This question, however, is beyond the scope of this report.

The crucial question to be answered here is whether a high recycling regime can be obtained also in the new, "hardened" ASDEX divertor knowing that it was established experimentally in the present divertor with both wide and narrow divertor slits. This is proven, if we find that for a given divertor plasma (obtained

by an appropriate choice of ϕ_E and ϕ_3 and a reasonable gettering assumption), the exit flux ϕ_{exit} and the gettering flux ϕ_{gett} (and hence ϕ_1) are sufficiently small compared to ϕ_3. More accurately if the flux amplification ϕ_3/ϕ_1 in the divertor is still of the order ten or higher, we believe that all the beneficial divertor effects (e.g. impurity control, acess to the H-mode etc.) are retained.

3. Results

The code package described above has been applied to three different ASDEX divertor geometries. Only the outer half of the upper divertor dome is treated in all cases.

a) The original standard divertor geometry, which is used at present (W: "wide" divertor slits; fig. 1a).

b) The standard divertor, but with inserts placed in the divertor slits to reduce the neutral gas conductance (N: "narrow" divertor slits).
This version was investigated experimentally for some period at ASDEX in order to check various physical models concerning the neutral gas balance and impurity retention /10/.

c) The divertor geometry after "hardening" (H; fig. 1b), which is a completely new design, the most obvious difference with respect to a) and b) being the divertor volume. The position of the divertor coil triplet is unchanged. This version is to be used for future long pulse heating.

In addition to these cases we have also treated two fictitious geometries (WH, NH), which are identical to a) and b), resp., except that the divertor volume was artificially reduced to the immediate neighbourhood of the plasma fan. Figure 2 shows these five cases (W, WH, N, NH and H) in the form used for the DEGAS neutral gas simulation. The dashed lines indicate flux surfaces within the plasma fan, the single solid line in between represents the separatrix. The density and temperature maximum is placed in the first cell at the right hand side of the separatrix, decaying gradually in the subsequent zones. A faster decay is assumed at the opposite side (see also ref. /11/). The plasma particles neutralized at the divertor plate form the source of neutral

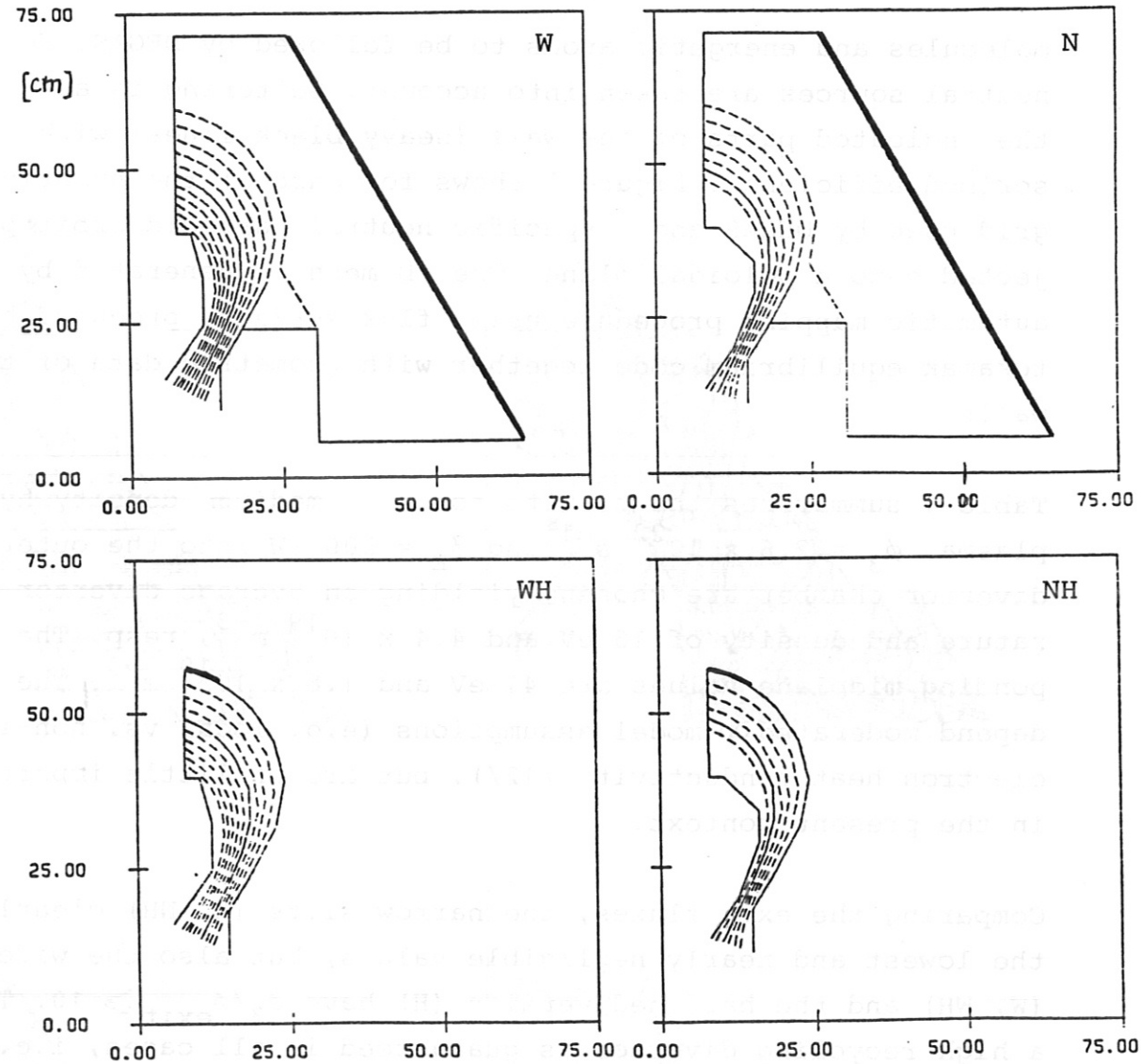

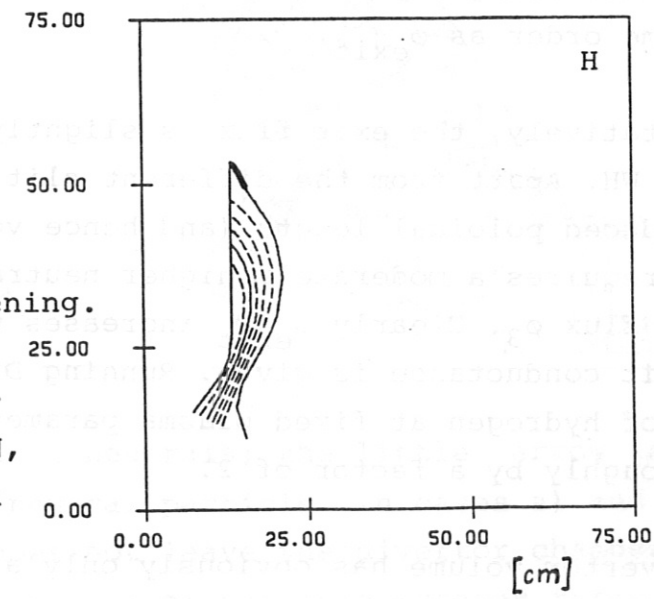

Fig. 2: Simulation of the ASDEX divertor chamber in DEGAS;

W: standard ASDEX

N: ASDEX divertor with narrow slits

H: ASDEX divertor after hardening.

WH and NH are fictitious geometries obtained from W and N, resp., by just cutting away a major part of the divertor volume outside the plasma fan (as an intermediate step between W or N and H).

molecules and energetic atoms to be followed by DEGAS. No other neutral sources are taken into account. Gettering is assumed at the indicated parts of the wall (heavy black lines) with a prescribed efficiency. Figure 3 shows for case a) the numerical grid used by DEGAS and specific neutral particle orbits projected onto a poloidal plane. The 2D mesh is generated by a semi-automatic mapping procedure using flux surfaces produced by a tokamak equilibrium code together with geometric data of the walls.

Table 1 summarizes the results for a medium density hydrogen plasma. $\phi_3 = 2.6 \times 10^{22}\ s^{-1}$ and $\phi_E = 500$ kW into the outer, upper divertor chamber are chosen, yielding an average divertor temperature and density of 16 eV and $4.4 \times 10^{19}\ m^{-3}$, resp. The corresponding midplane values are 41 eV and $1.8 \times 10^{19}\ m^{-3}$. The latter depend moderated on model assumptions (e.g. local vs. non-local electron heat conductivity /12/), but are of little importance in the present context.

Comparing the exit fluxes, the narrow slits (N, NH) clearly yield the lowest and nearly negligible values, but also the wide slits (W, WH) and the hardened version (H) have $\phi_3/\phi_{exit} \geqslant 10$. Therefore, a high recycling divertor is guaranteed in all cases, i.e. also after "hardening", provided that the gettering flux is at most of the same order as ϕ_{exit}.

Quantitatively, the exit flux is slightly higher for case H than for W, WH. Apart from the different slit geometry, one reason is the reduced poloidal length (and hence volume) of the plasma fan, which requires a moderately higher neutral density to sustain the target flux ϕ_3. Clearly ϕ_{exit} increases with neutral density, if the slit conductance is given. Running DEGAS with deuterium instead of hydrogen at fixed plasma parameters decreases the exit flux roughly by a factor of 2.

The divertor volume has obviously only a small influence on the particle loss (W, N vs. WH, NH). However, it determines the total number of neutrals N_o in the divertor (counted in atoms), since

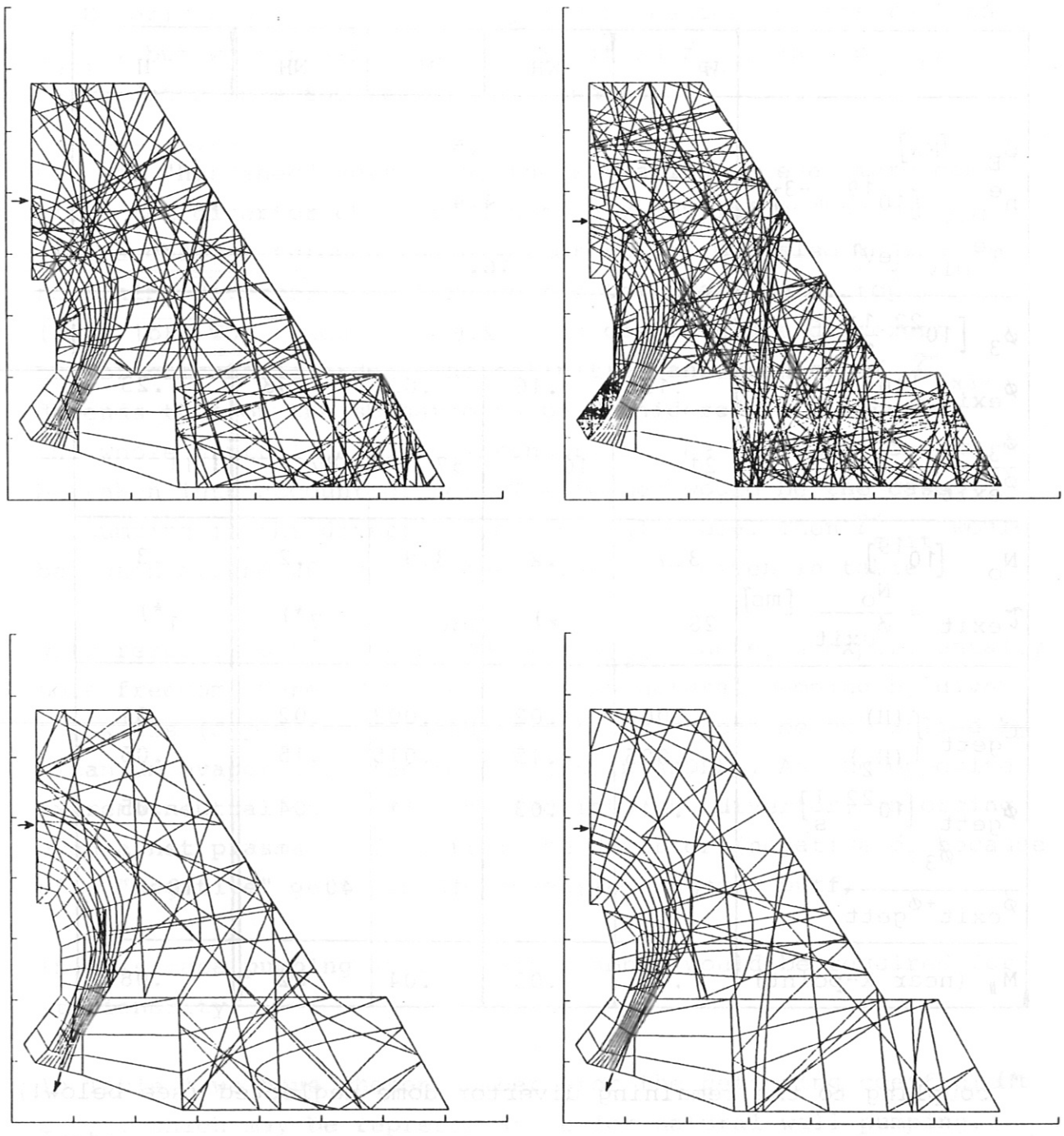

Fig. 3: DEGAS test flights of neutrals; the little arrow indicates the origin of the neutral particle. In cases a) and b) the neutral particle does not leave the divertor chamber; in cases c) and d), the neutral particle escapes through the slit.

Table 1

	W	WH	N	NH	H
ϕ_E [MW]	.5				
n^e_{Div} [10^{19} m^{-3}]	4.4				
T^e_{Div} [eV]	16.				
ϕ_3 [10^{22} $\frac{1}{s}$]	2.6				
ϕ_{exit} [10^{22} $\frac{1}{s}$]	.13	.16	.03	.03	.23
$\frac{\phi_3}{\phi_{exit}}$	21	16	87	87	11
N_o [10^{19}]	3.7	.2	3.9	.2	.3
$\tau_{exit} = \frac{N_o}{\phi_{exit}}$ [ms]	28	1*)	130	7*)	1*)
C_{gett} (H)	.001	.02	.003	.02	.01
C_{gett} (H_2)	.005	.15	.015	.15	.05
ϕ_{gett} [10^{22} $\frac{1}{s}$]	.04	.03	.11	.04	.05
$\frac{\phi_3}{\phi_{exit}+\phi_{gett}}$	16	13	18	40	10
$M_{\parallel}$ (near X-point)	.05	.05	.04	.02	.08

*) coupling to the remaining divertor dome neglected (see below!)

the neutral density is roughly the same. The volume enters also into the neutral gas divertor constant $\tau_{exit} = N_o/\phi_{exit}$, which therefore is a factor of 20 smaller for H compared to W. Experimentally, τ_{exit} and n_o may be easier to measure than ϕ_{exit}, but we emphasize again that it is ϕ_{exit} (and ϕ_{gett}) which determines the recycling intensity.

For the "hardened" version H, the situation is even more complex: the divertor chamber is not only coupled to the main plasma chamber through the divertor slits, but also to the remaining divertor dome through the toroidal gap on top (fig. 1b). The conductances of both openings are different but of comparable order. The definition and meaning of τ_{exit} depends then on the scenario to be considered, e.g. whether the whole neutral particle inventory in the divertor dome must be taken into account or not. The former would be the case, if pumping in the divertor dome is negligible. Then τ_{exit} would be again around 20 ms instead of the 1 ms given in table 1.

With respect to the gettering flux ϕ_{gett} there is experimentally more freedom. Generally there is some natural pumping by divertor walls (depending on saturation), which can be multiplied by titanium evaporation (up to 10^6 1/s in ASDEX). As the opposite extreme neutral gas can be puffed into the divertor, enforcing even a net plasma outflow from the divertor (negative ϕ_1 because of a "negative" gettering representing the gas puff).

In this case pumping in the main chamber would be required for stationarity.

In Table 1 we have chosen numbers for the gettering coefficient c_{gett}, which may be representative for natural wall pumping, resulting in ϕ_{gett} of the same order as ϕ_{exit}. Variations to both sides are possible, but since this flux can be experimentally controlled to some extent, it is not of crucial importance here. By variation of the pumping the total particle multiplication $\phi_3/(\phi_{exit} + \phi_{gett})$ and the flow velocity along field lines and

the average Mach number $M_{//}$ outside the divertor can be also controlled within limits.

For the "hardened" divertor (H) there is a toroidal gap at the top of the divertor chamber (Fig. 1b), which links the divertor with the remaining divertor dome volume, where titanium gettering can still be applied. Depending on the degree of gettering in this supplementary volume, a pressure will build up and some particles return into the active divertor volume. In the simulation this is represented by an appropriately chosen gettering coefficient at the gap area (in cases H, WH, NH). The effect on τ_{exit} has been discussed already above.

In order to show the density dependence, we have repeated the simulations with a higher and a lower divertor density at roughly the same divertor temperature, i.e. by varying ϕ_3 and ϕ_E, keeping ϕ_E/ϕ_3 approximately constant as discussed earlier. The results are summarized in Tables 2 and 3: Lowering the divertor density, the ratio ϕ_3/ϕ_{exit} reduces to $\lesssim 10$ for W, WH and especially for H (table 2). Nevertheless, an appreciable recycling is still retained as long as the gettering flux is small enough, and the mass flow outside the divertor chamber is still subsonic ($M_{//} \leq 0.13$). For even lower density or increased gettering, however, the high recycling regime becomes questionable.

If the density is increased by a factor of three, then the divertor slits are effectively blocked ($\phi_{exit} \ll \phi_3$) and the plasma inflow ϕ_1 is low and partly determined by the gettering flux ϕ_{gett} (table 3).

A temperature variation at constant divertor density does not cause so strong changes as long as the temperature in the slit region remains above the hydrogen ionization threshold.

Finally table 4 summarizes the comparison of the two experimentally most relevant geometries (W and H) with respect to the exciting flux of neutrals ϕ_{exit} for the three power cases. In addition, profiles along field lines for W and H are given in the appendix.

Table 2

	W	WH	N	NH	H
ϕ_E [MW]	.15				
n^e_{Div} [10^{19} m^{-3}]	1.2				
T^e_{Div} [eV]	19				
ϕ_3 [10^{22} $\frac{1}{s}$]	.7				
ϕ_{exit} [10^{22} $\frac{1}{s}$]	.07	.13	.02	.04	.16
$\frac{\phi_3}{\phi_{exit}}$	10	5	35	18	4
N_o [10^{19}]	1.5	.09	1.8	.09	.14
$\tau_{exit} = \frac{N_o}{\phi_{exit}}$ [ms]	20	1	68	3	1
C_{gett} (H)	.001	.02	.003	.02	.01
C_{gett} (H_2)	.005	.15	.015	.15	.05
ϕ_{gett} [10^{22} $\frac{1}{s}$]	.016	0.014	0.05	.017	.02
$\frac{\phi_3}{\phi_{exit}+\phi_{gett}}$	8	5	10	12	4
$M_{//}$ (near X-point)	.07	.10	.05	.04	.13

Table 3

	W	WH	N	NH	H
ϕ_E [MW]	1.5				
n^e_{Div} [10^{19} m^{-3}]	12.6				
T^e_{Div} [eV]	17				
ϕ_3 [10^{22} $\frac{1}{s}$]	8.7				
ϕ_{exit} [10^{22} $\frac{1}{s}$]	.07	.08	.01	.01	.16
$\frac{\phi_3}{\phi_{exit}}$	124	109	870	870	54
N_o [10^{19}]	8	.4	8	.4	.61
exit $= \frac{N_o}{\phi_{exit}}$ [ms]	116	5	824	65	4
C_{gett} (H)	.001	.02	.003	.02	.01
C_{gett} (H_2)	.005	.15	.015	.15	.05
ϕ_{gett} [10^{22} $\frac{1}{s}$]	.07	.09	.22	.11	.11
$\frac{\phi_3}{\phi_{exit}+\phi_{gett}}$	60	50	35	70	32
$M_{\parallel}$ (near X-point)	.01	.02	.02	.01	.02

Table 4

	$\phi_{exit}\ [10^{22}\ \frac{1}{s}]$	
	W	H
$\phi_E = .15\ [MW]$ $\phi_3 = .7 \times 10^{22}[\frac{1}{s}]$	.07	.16
$\phi_E = .50\ [MW]$ $\phi_3 = 2.6 \times 10^{22}[\frac{1}{s}]$	.13	.23
$\phi_E = 1.50\ [MW]$ $\phi_3 = 17. \times 10^{22}[\frac{1}{s}]$	.07	.16

We emphasize, however, that for the present study classical electron heat conduction along field lines was assumed and charge exchange friction in the divertor chamber was not yet included. If, for example, long mean free path effects are included, then the midplane plasma parameters may change appreciably as shown in ref. /12/.

Acknowledgement

We are grateful to the authors of "DEGAS" (PPPL) for providing their code and to Dr. K.G.Rauh for his assistance with the coupling of DEGAS and SOLID.

References

/1/ G. Fußmann et al., J. Nucl. Mat. 128 & 129, 350 (1984)

/2/ W. Engelhardt et al., J. Nucl. Mat. 111 & 112, 337 (1982)

/3/ M. Keilhacker et al., "Plasma Physics and Contr. Nucl. Fusion Research 1982", Vol. III, p. 183, IAEA, Vienna 1983 (Proceedings of the IAEA Conference, Baltimore, USA)

/4/ IPP Annual Report 1984 ASDEX-Projekt (§ 4.2)

/5/ O. Gruber et al., J. Nucl. Mat. 121, 407 (1984)

/6/ W. Schneider et al., J. Nucl. Mat. 121, 178 (1984)

/7/ D. Heifetz et al., J. Comput. Phys. 46 (1982), 309

/8/ K. Lackner et al., Plasma Physics and Controlled Fusion 26 (No. 1A), 105 (1984)

/9/ Shimomura et al., Nucl. Fusion 23, 869 (1983)

/10/ G. Fußmann et al., J. Nucl. Mat. 121, 164 (1984)

/11/ D. Heifetz et al., Contr. Fusion and Plasma Physics, Aachen 1983, Vol. 7D, part II, p. 239 (A 34)

/12/ K. Lackner et al., Plasma Physics and Contr. Nucl. Fusion Research, London 1984, Vol. 1, p. 319.

Appendix: Profiles along field lines

In addition to the global data given in the main text, in Figs. 4, 5, and 6, plasma and neutral gas profiles along the field lines are shown for the three different power fluxes. In the (a)-figures the results for the standard ASDEX geometry (W) are plotted; whereas the (b)-figures show the corresponding results for the hardened divertor (H).

The four upper plots are the plasma quantities as function of s ($o \leq s \leq 15$ m): electron density n_e [m^{-3}], plasma temperatures kT_e, kT_i [eV], particle flux [1/s], and power fluxes [W].

The four lower graphs show the profiles of plasma density and temperature ($kT_{e,i}$) and the particle density n_H [m^{-3}] and temperature kT_H[eV] of the neutral atoms within the divertor chamber (10 m $\leq s \leq$ 15 m).

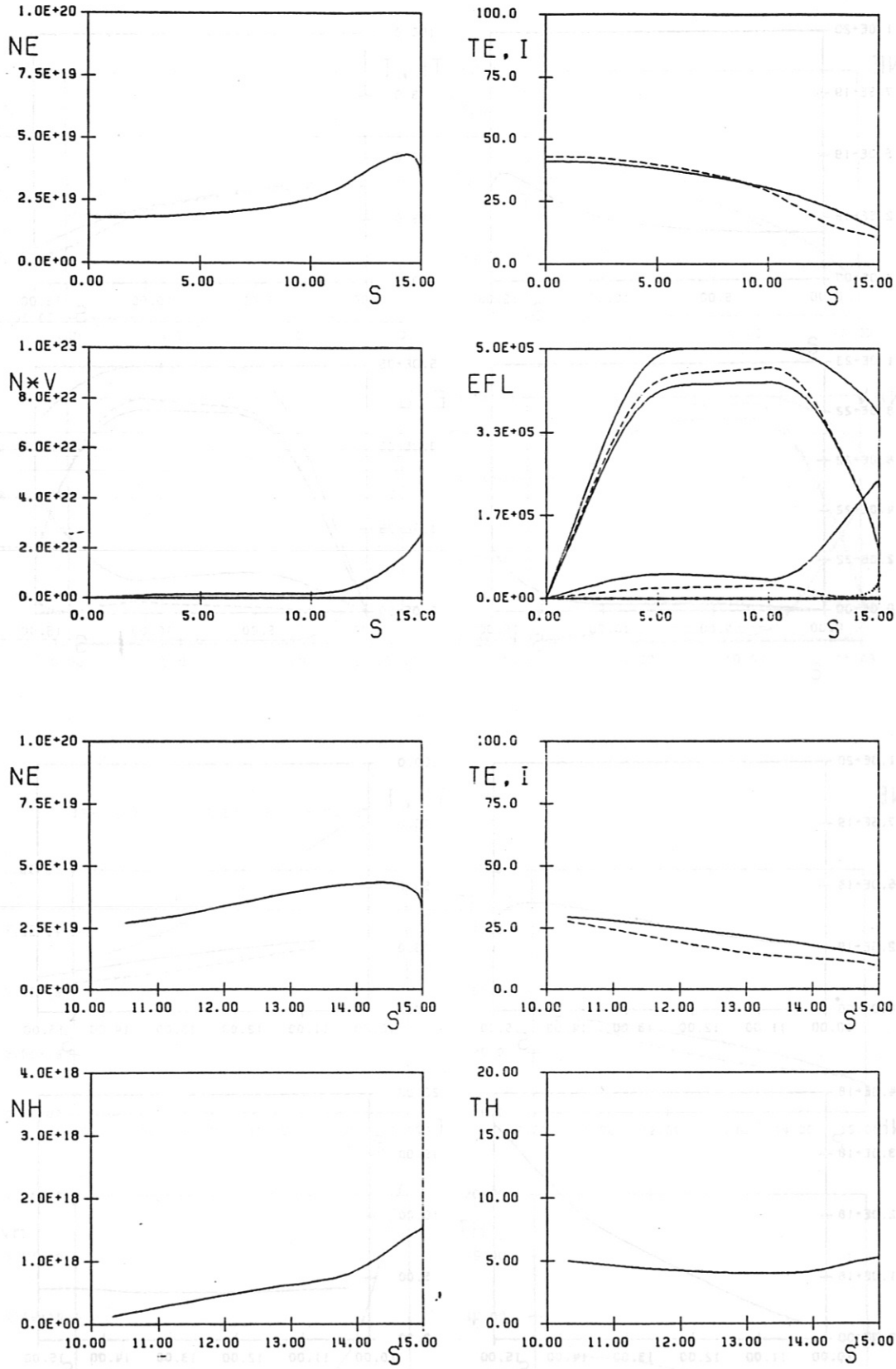

Fig. 4a: Plasma and neutral gas profiles
ASDEX W-geometry; ϕ_E = .5 MW.

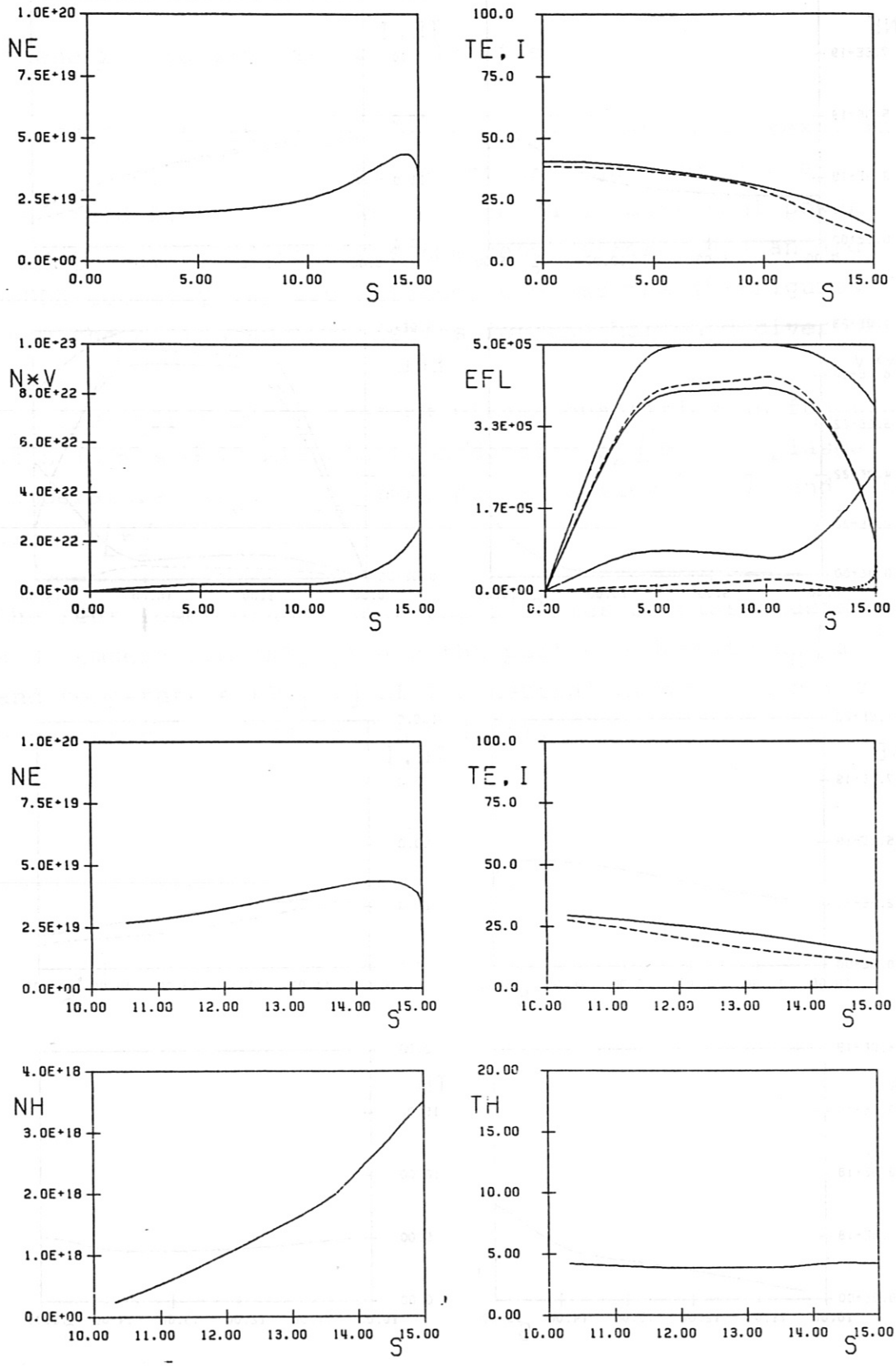

Fig. 4b: Plasma and neutral gas profiles
ASDEX H-geometry; ϕ_E = .5 MW.

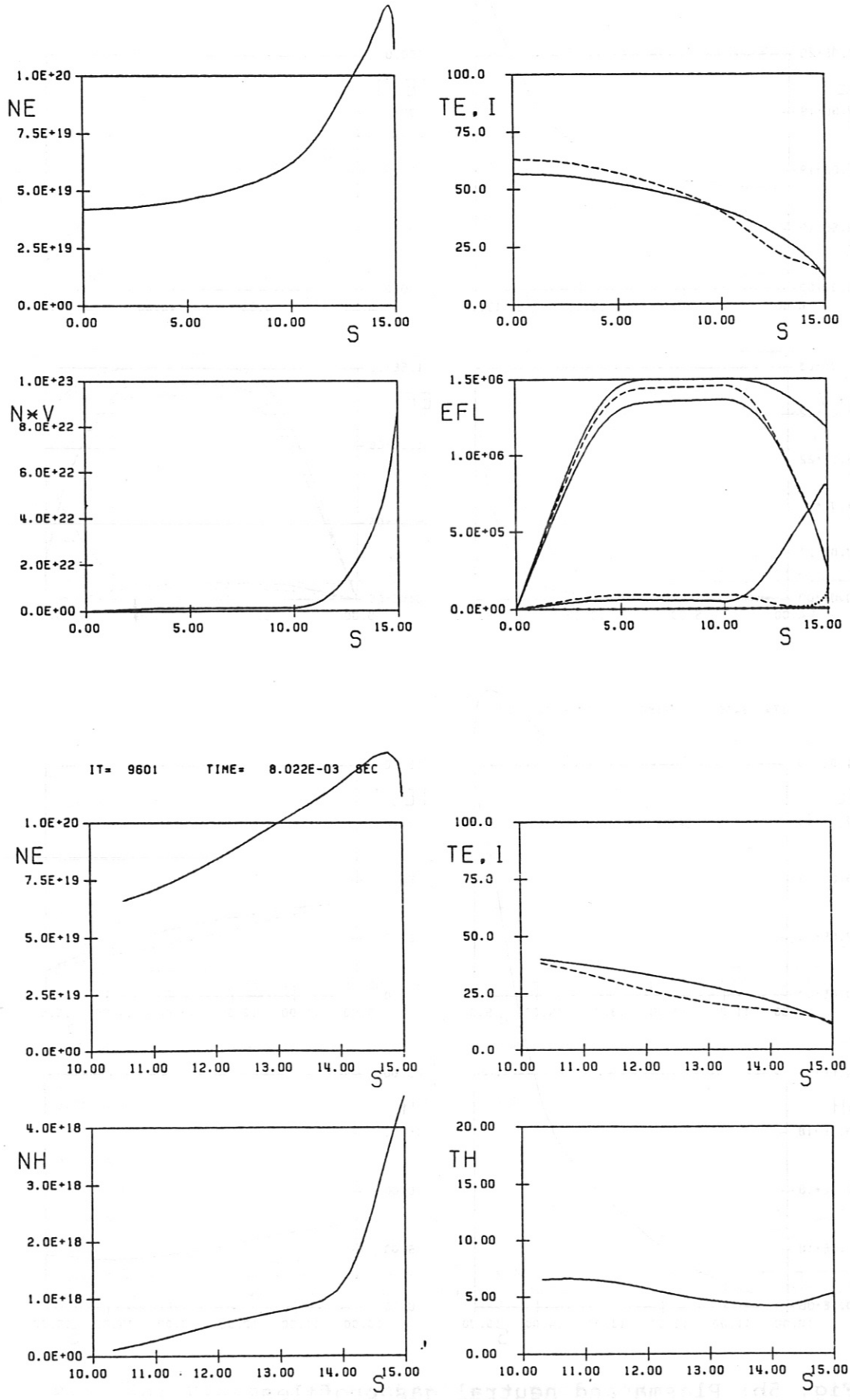

Fig. 5a: Plasma and neutral gas profiles
ASDEX W-geometry; ϕ_E = 1.5 MW.

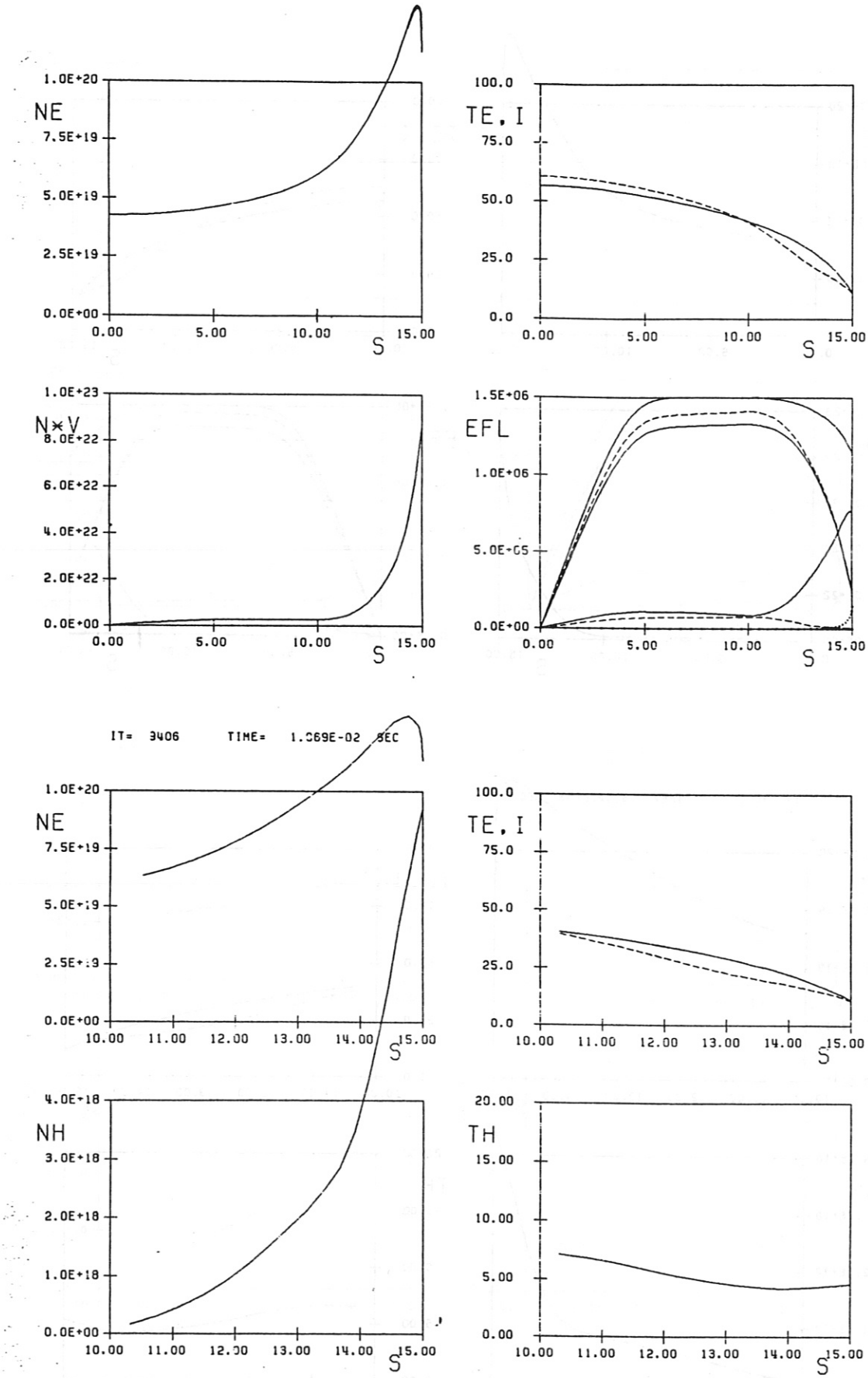

Fig. 5b: Plasma and neutral gas profiles
ASDEX H-geometry; ϕ_E = 1.5 MW.

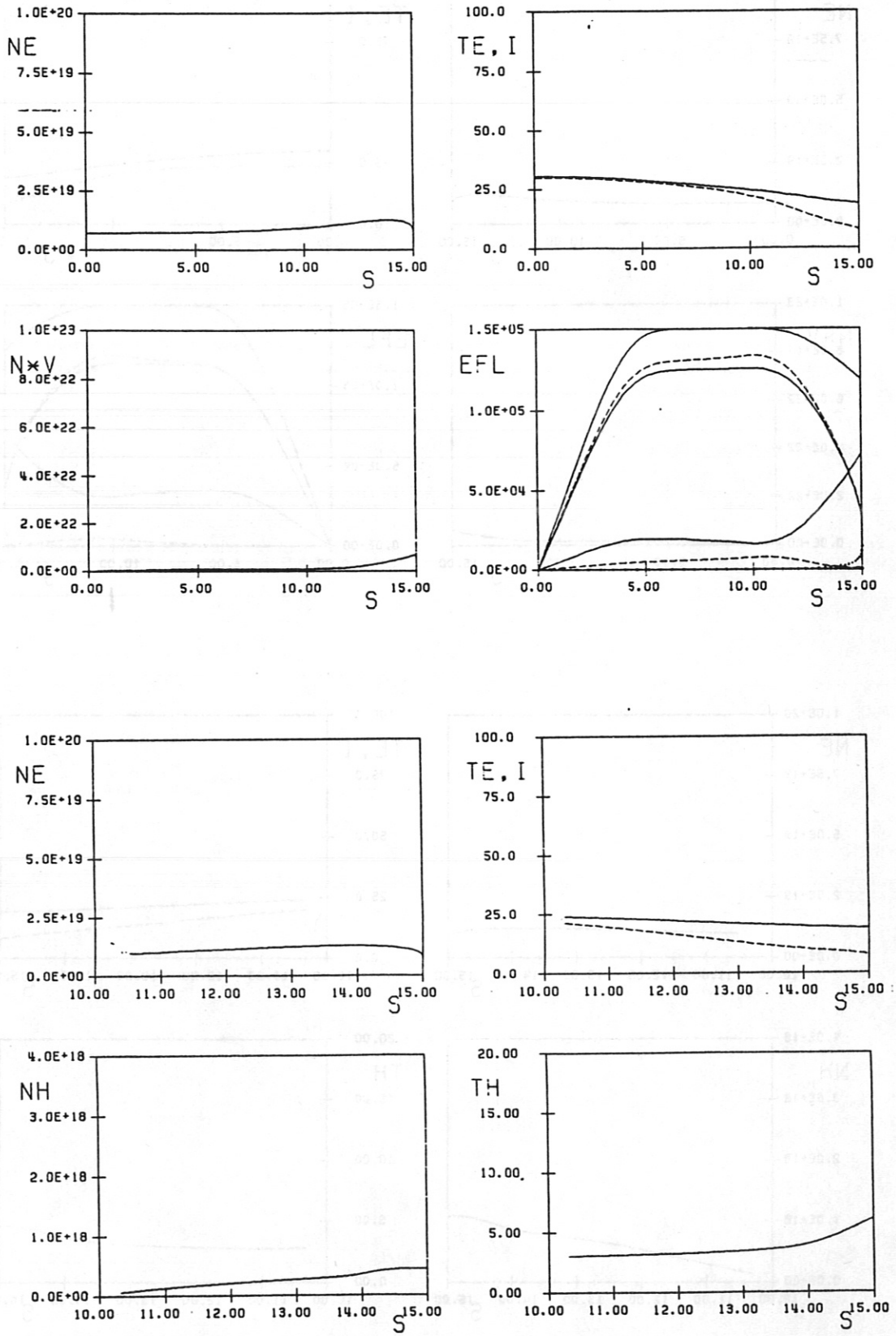

Fig. 6a: Plasma and neutral gas profiles
ASDEX W-geometry; ϕ_E = .15 MW.

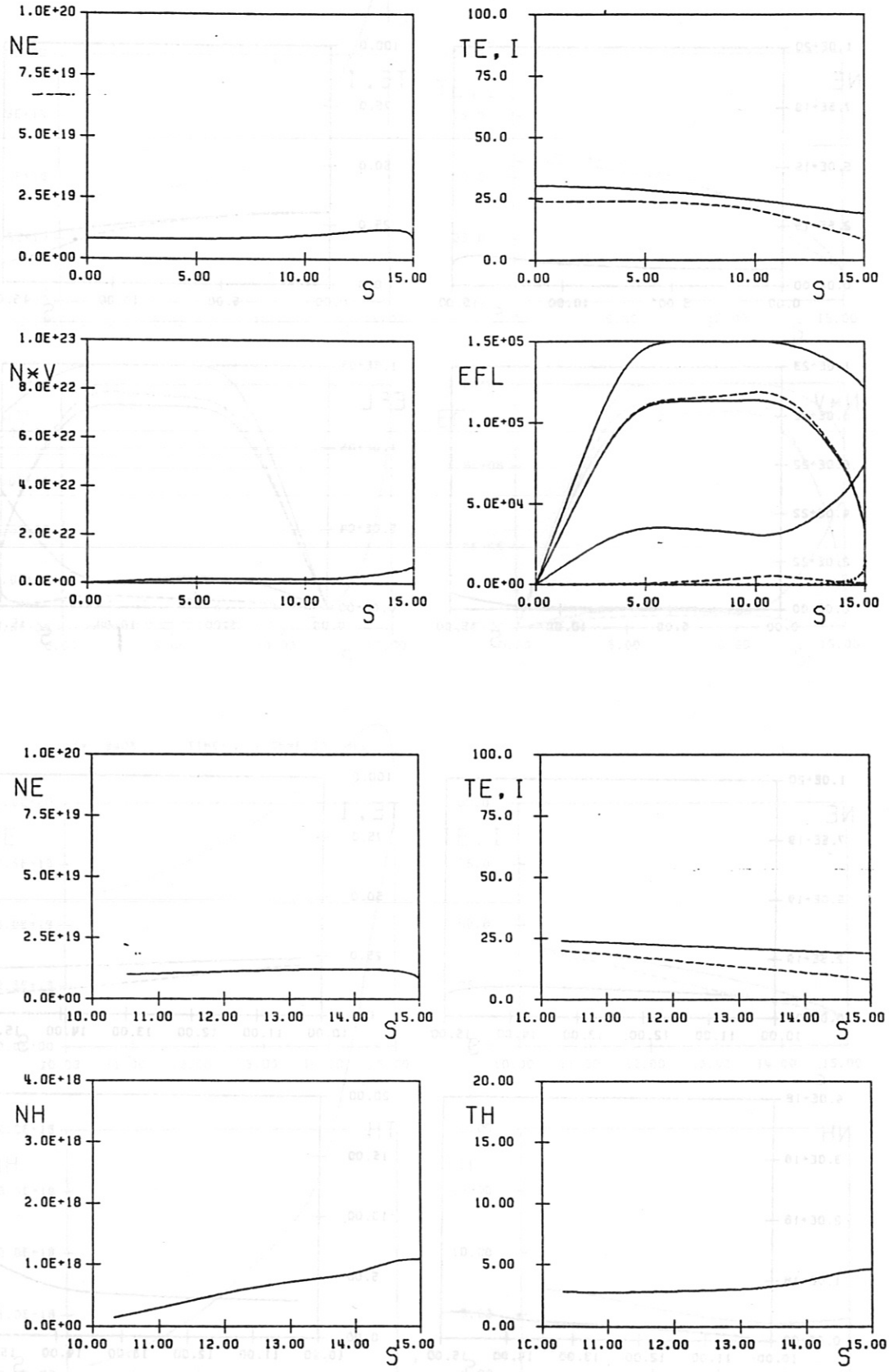

Fig. 6b: Plasma and neutral gas profiles
ASDEX H-geometry; ϕ_E = .15 MW.